

**A  $\pm$  12-A High-Side Current Sensor With 25 V Input CM Range and 0.35% Gain Error From  $-40$  °C to  $85$  °C**

Xu, Long; Heidary Shalmany, Saleh; Huijsing, Johan H.; Makinwa, Kofi

**DOI**

[10.1109/LSSC.2018.2855407](https://doi.org/10.1109/LSSC.2018.2855407)

**Publication date**

2018

**Document Version**

Accepted author manuscript

**Published in**

IEEE Solid State Circuits Letters

**Citation (APA)**

Xu, L., Heidary Shalmany, S., Huijsing, J. H., & Makinwa, K. (2018). A  $\pm$  12-A High-Side Current Sensor With 25 V Input CM Range and 0.35% Gain Error From  $-40$  °C to  $85$  °C. *IEEE Solid State Circuits Letters*, 1(4), 94-97. <https://doi.org/10.1109/LSSC.2018.2855407>

**Important note**

To cite this publication, please use the final published version (if applicable). Please check the document version above.

**Copyright**

Other than for strictly personal use, it is not permitted to download, forward or distribute the text or part of it, without the consent of the author(s) and/or copyright holder(s), unless the work is under an open content license such as Creative Commons.

**Takedown policy**

Please contact us and provide details if you believe this document breaches copyrights. We will remove access to the work immediately and investigate your claim.

# A $\pm 12\text{A}$ High-Side Current Sensor with 25V Input CM Range and 0.35% Gain Error from $-40^\circ\text{C}$ to $85^\circ\text{C}$

Long Xu, *Student Member, IEEE*, Saleh Heidary Shalmany, *Student Member, IEEE*,  
 Johan H. Huijsing, *Life Fellow, IEEE* and Kofi A. A. Makinwa, *Fellow, IEEE*

**Abstract**—This paper presents the most accurate shunt-based high-side current sensor ever reported. It achieves a 25V input common-mode range from a single 1.8V supply by using a beyond-the-rails ADC. A hybrid analog/digital temperature compensation scheme is proposed to simplify the circuit implementation while maintaining the state-of-the-art accuracy. Over a  $\pm 12\text{A}$  current range, the sensor exhibits 0.35% gain error from  $-40^\circ\text{C}$  to  $85^\circ\text{C}$  with 3x better power efficiency.

**Index Terms**—Current sensor, high-side current sensing, high voltage, shunt resistor, temperature sensor, temperature compensation,  $\Delta\Sigma$  ADC.

## I. INTRODUCTION

Accurate current sensing is critical in many applications including battery management, motor control and over-current protection. The most common and simple approach for current sensing is the use of a shunt resistor. Based on where the shunt resistor is placed, two approaches can be identified: low-side current sensing and high-side current sensing (Fig. 1). Compared to low-side current sensing, high-side current sensing does not increase the resistance of the ground path and enables robust short-circuit detection. However, the challenge associated with high-side current sensing is that it requires high-voltage (HV) interface circuits to accommodate large input CM voltages. Such circuits typically consist of HV instrumentation amplifiers (IA) [1] that translate HV signals down to low voltage domain where they are digitized by a conventional ADC. In this design, a HV beyond-the-rails ADC [2] is used to directly digitize HV signals, thus obviating the need for HV IAs, and reducing both chip area and power.

To build fully integrated low-cost current sensors, shunt resistors can be realized with either metal layers of a CMOS process, or the lead-frame of a plastic package [3]. In both cases, shunt resistance will vary with temperature, thus requiring a temperature compensation scheme (TCS) for good accuracy. Unlike the digital TCS in [3] which requires a relatively accurate temperature sensor (TS), this design proposes a hybrid analog/digital TCS to greatly relax the required accuracy of the TS while maintaining the state-of-the-art accuracy. Furthermore, it also provides flexible current-sensing accuracy in different operation modes depending on different applications.

This paper is organized as follows. Section II describes the system architecture and circuit implementation of the sensor. Experimental results are presented in Section III and Section IV concludes the paper.

Manuscript received xx x, 2018;

L. Xu, J. H. Huijsing and K. A. A. Makinwa are with the Microelectronics Department, Delft University of Technology, 2628 CD Delft, The Netherlands (e-mail: l.xu-1@tudelft.nl).

S. H. Shalmany is with SiTime, 2612 PA Delft, The Netherlands.

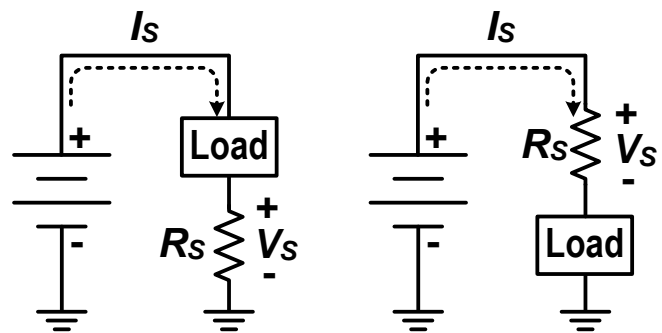


Fig. 1. Low-side current sensing (left) and high-side current sensing (right).

## II. SENSOR ARCHITECTURE

### A. System Overview

Fig. 2 shows the system architecture of the sensor. It consists of a shunt resistor  $R_s$  ( $\sim 1\text{m}\Omega$ ) made from a copper PCB trace, a HV beyond-the-rails ADC, a TS and a reference voltage generator (RVG).

For rapid prototyping, a PCB trace is used to emulate the lead-frame shunt used in [3]. Compared to an on-chip metal shunt [4], it enables a  $\pm 12\text{A}$  current sensing range with no extra silicon area cost, which is 3x wider than [4]. Good thermal coupling and galvanic isolation are achieved by directly bonding the chip to the trace with non-conductive glue. The HV ADC digitizes the voltage drop across the shunt  $V_s$  via Kelvin contacts S1 & S2 (Fig. 3) with regard to the voltage reference  $V_{\text{PTAT}}$  generated from the RVG. Meanwhile, the TS senses the shunt's temperature, whose output  $\mu\text{T}$  is used to correct the digitized shunt voltage  $\mu\text{I}$  with the help of a single 2<sup>nd</sup>-order polynomial.

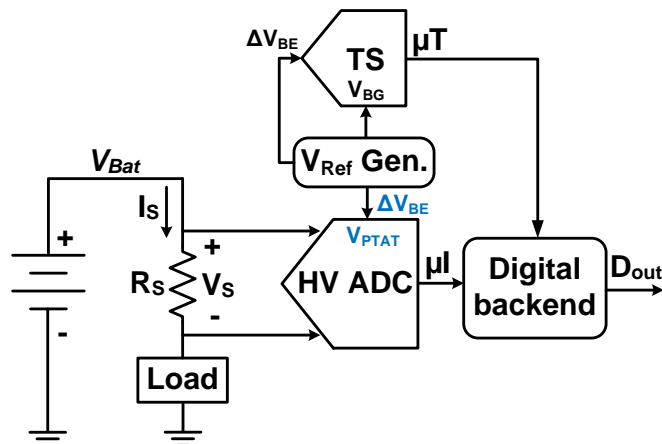


Fig. 2. System architecture of the sensor.

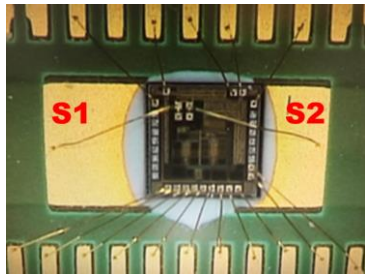


Fig. 3. Bonding diagram of the chip.

### B. Beyond-the-rails ADC

Fig. 4 shows the schematic of the HV beyond-the-rails ADC. It is based on a 2<sup>nd</sup>-order switched-capacitor  $\Delta\Sigma$  ADC. A HV chopper  $CH_{HV}$  [2] ensures that the voltage across the shunt  $V_S$  is sampled by capacitors  $C_{S1}$  (2pF) in a cross-coupled fashion such that they block the input CM voltage. In a similar manner, the reference  $V_{PTAT}$  is sampled onto feedback capacitors  $C_{S2}$ . Both  $C_{S1}$  and  $C_{S2}$  are implemented as HV fringe capacitors with a breakdown voltage of 70V. In this design  $C_{S2} = C_{S1}/2$ , which reduces the equivalent reference voltage and ensures that the chosen  $\pm 12A$  current range corresponds to  $\sim 60\%$  of the ADC's dynamic range (DR). This contrasts favorably with [3], in which only 10% of the ADC's DR is utilized. It improves the ADC's power efficiency by reducing the integrators' output swing, the  $kT/C$  noise contribution from its feedback branch, and the capacitive load of the 1<sup>st</sup> integrator. In addition, the ADC's loop filter is realized with energy-efficient current-reuse amplifiers. Correlated double sampling and low-frequency chopping (CHL) are employed in the ADC to suppress offset and  $1/f$  noise. For simplicity, CHL is realized by logically controlling the states of a single HV input chopper.

The schematic of the HV chopper is shown in Fig. 5. Clock signals  $\Phi 1$ ,  $\Phi 2$  are capacitively-coupled to the gates of four switches  $M_{1-4}$  via a level shifter composed of two HV capacitors  $C_{1-2}$  and a latch  $M_{5-6}$ . A minimum selector  $M_{S1-2}$  ensures that coupled clocks are always superimposed on the  $V_{min}$  (the lower of  $V_{ip}$  and  $V_{in}$ ), which minimizes the leakage current of  $M_{1-4}$  in the presence of bidirectional input voltages.

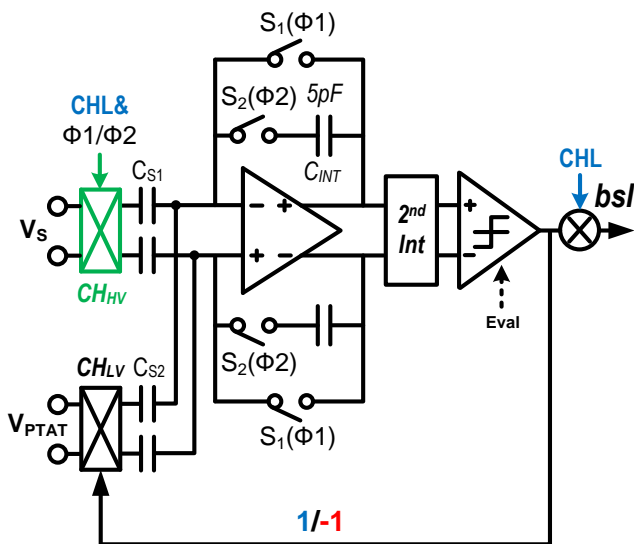


Fig. 4. Schematic of the beyond-the-rails ADC.

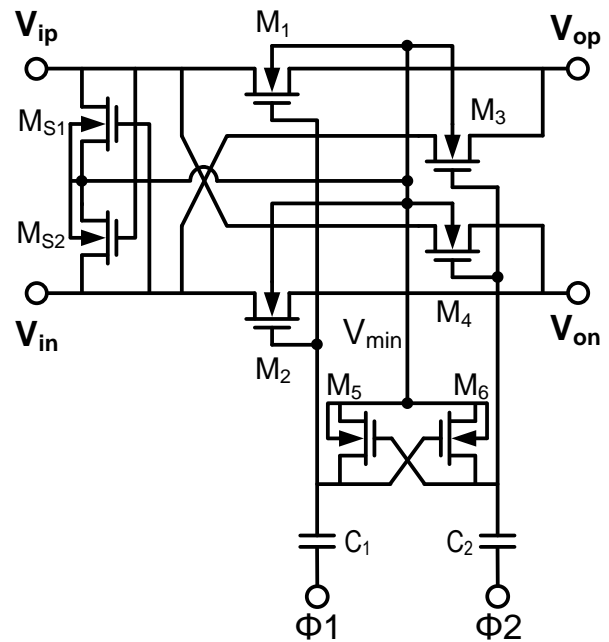


Fig. 5. Simplified schematic of the HV chopper.

### C. Hybrid analog/digital temperature compensation scheme

In [3], the shunt voltage  $V_S$  is digitized by an ADC with respect to a nearly temperature-independent bandgap reference. An on-chip TS then senses the shunt's temperature such that its temperature dependency can be compensated in the digital domain. Since copper has a relatively large temperature coefficient of resistance (TCR  $\sim 0.38\%/^{\circ}C$ ), the TS has to achieve an inaccuracy of less than  $0.5^{\circ}C$  in order not to become a dominant error source.

In this design, instead of a bandgap reference, a proportional-to-absolute-temperature (PTAT) voltage  $V_{PTAT}$  is employed as the ADC's reference [4]. Since the shunt resistance's temperature dependency is also roughly PTAT, it is effectively compensated by the TC of  $V_{PTAT}$ , thus realizing an analog TCS. However, since the shunt resistance's temperature dependency is non-linear and not perfectly PTAT, there will still be some residual error. This can be modelled by a fixed 2<sup>nd</sup>-order polynomial and then digitally corrected with the help of the TS. Noting that the TC of this residual error is 8x less than that of copper, the TS's accuracy can be relaxed for the same current sensing accuracy.

Fig. 6 shows the schematic of the RVG and the TS. Two vertical NPN transistors are biased at a current density ratio of 7. The base-emitter voltage difference  $\Delta V_{BE}$  of two NPN transistors is PTAT, and is used as the ADC's reference  $V_{PTAT}$ . Since a bandgap reference is not necessary, no  $V_{BE}$  sampling capacitors are required in the ADC (Fig. 4), unlike [3]. This avoids errors due to capacitor mismatch and  $V_{BE}$  curvature. Dynamic element matching of the NPNs and CHL for TS are eliminated in this design due to the relaxed requirement on the TS accuracy. The current sources are chopped to suppress their  $1/f$  noise.

The TS digitizes the shunt's temperature by charge-balancing  $\Delta V_{BE}$  against  $-V_{BE}/10$  [3]. When  $bsT$  is 0,  $C_{S3}$  ( $= 1pF$ ) samples  $+\Delta V_{BE}$  and when  $bsT$  is +1,  $C_{S4}$  ( $= 100fF$ ) samples  $-V_{BE}$ . This results in an average value of  $bsT$  ( $\mu T$ ) equal to  $\Delta V_{BE} / (\Delta V_{BE} + V_{BE}/10)$  ( $(\Delta V_{BE} + V_{BE}/10)$  generates a bandgap reference), which is a linear function of temperature.

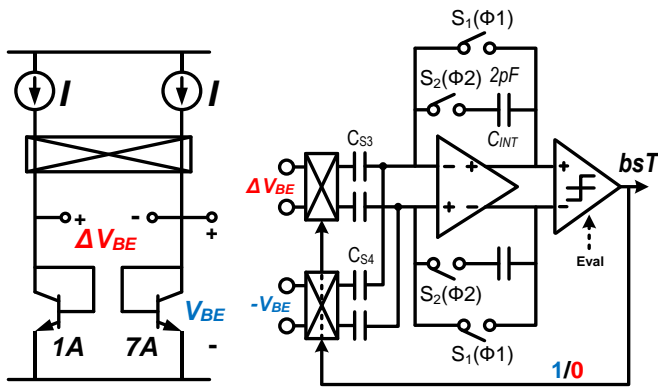


Fig. 6. Schematic of the RVG (left) and the TS (right).

### III. EXPERIMENTAL RESULTS

The sensor is fabricated in a  $0.18\mu\text{m}$  HV BCD CMOS technology with a core area of  $1.4\text{mm}^2$  (Fig. 7). At room temperature, it draws  $13.8\mu\text{A}$  from a  $1.8\text{V}$  supply. At a  $200\text{-kHz}$  sampling frequency and for a conversion time of  $12.5\text{ms}$ , the ADC and TS achieve resolutions of  $1.1\mu\text{V}_{\text{rms}}$  and  $10\text{mK}_{\text{rms}}$  respectively.

Fig. 8 shows the variation of the ADC's bit-stream average  $\mu I$  over temperature. For a constant input current ( $1\text{A}$ ),  $\mu I$  varies by  $\pm 28\%$  from  $-40^\circ\text{C}$  to  $85^\circ\text{C}$  due to the large TCR of the copper shunt when the bandgap reference is used. This drops to  $\pm 3.5\%$  when the PTAT reference  $V_{\text{PTAT}}$  is used. Without the TCS, the sensor only achieves a gain error of  $30\%$  (1 sample) from  $-40^\circ\text{C}$  to  $85^\circ\text{C}$  (Fig. 9). The use of a PTAT reference (analog TCS) reduces this to  $3.8\%$  (8 samples) (Fig. 10), which is further reduced to  $0.35\%$  when the output of the ADC is digitally corrected (Fig. 11). Each sensor is individually trimmed (at  $\sim 23^\circ\text{C}$  and  $4\text{A}$ ) to correct the spread of the shunt's nominal resistance. From  $-40^\circ\text{C}$  to  $85^\circ\text{C}$  and over a  $25\text{V}$  input CM range (ICMR), the ADC exhibits a maximum offset of  $24\mu\text{V}$ , which drops below  $1\mu\text{V}$  after applying CHL (Fig. 12). The measured inaccuracy of the TS is  $\pm 1.2^\circ\text{C}$  without trimming (Fig. 13), which is quite relaxed ( $2.5\times$  worse) compared to the TS used in [3].

The performance of the sensor is summarized in Table I. Among high-side current sensors [4]-[5], this design achieves the best accuracy. Compared to [3], it achieves similar accuracy,  $3\times$  better power-efficiency and  $30\times$  wider ICMR, by using a beyond-the-rails ADC and a hybrid TCS.

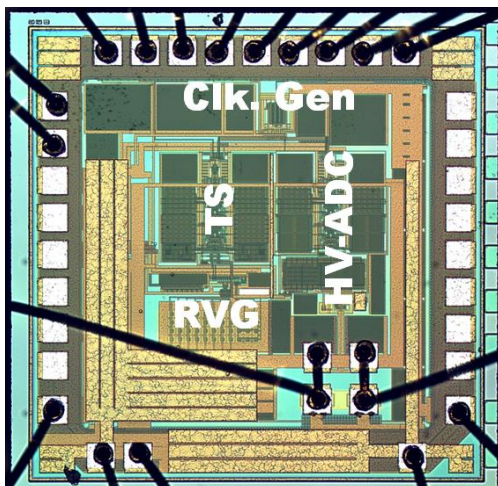


Fig. 7. Chip photo.

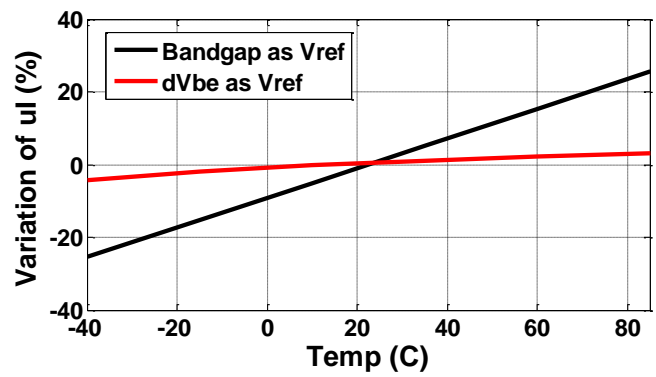


Fig. 8. Variation of  $\mu I$  over temperature.

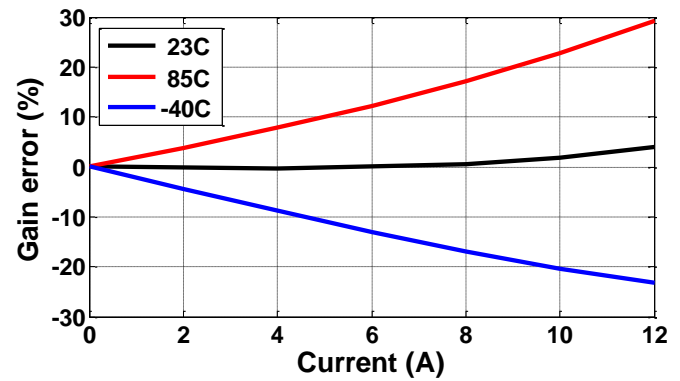


Fig. 9. Current sensing gain error without TCS.

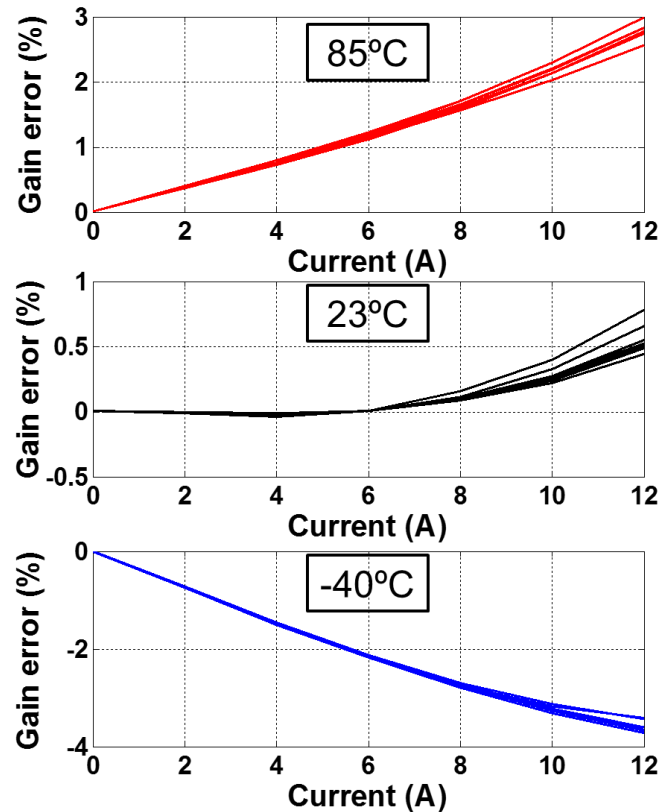


Fig. 10. Current sensing gain error with only analog TCS.

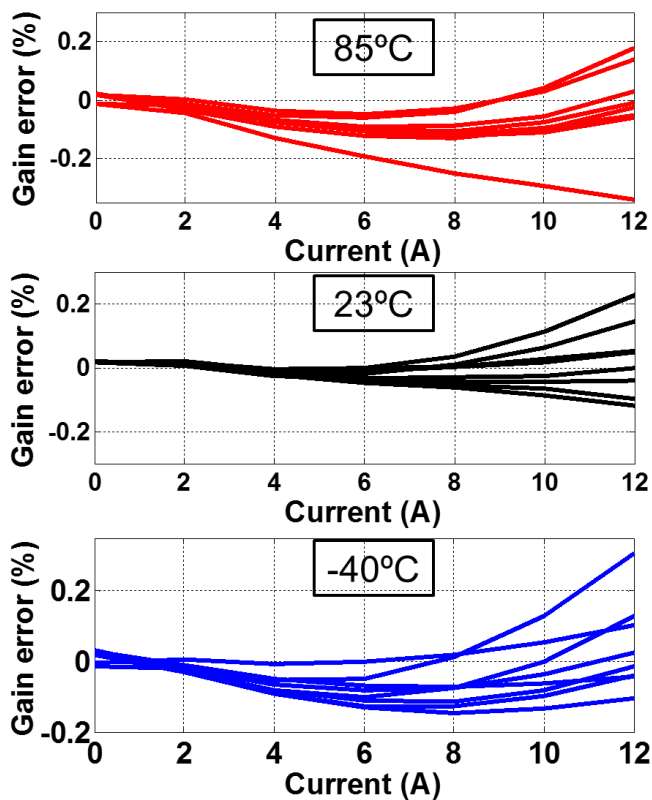


Fig. 11. Current sensing gain error with hybrid TCS.

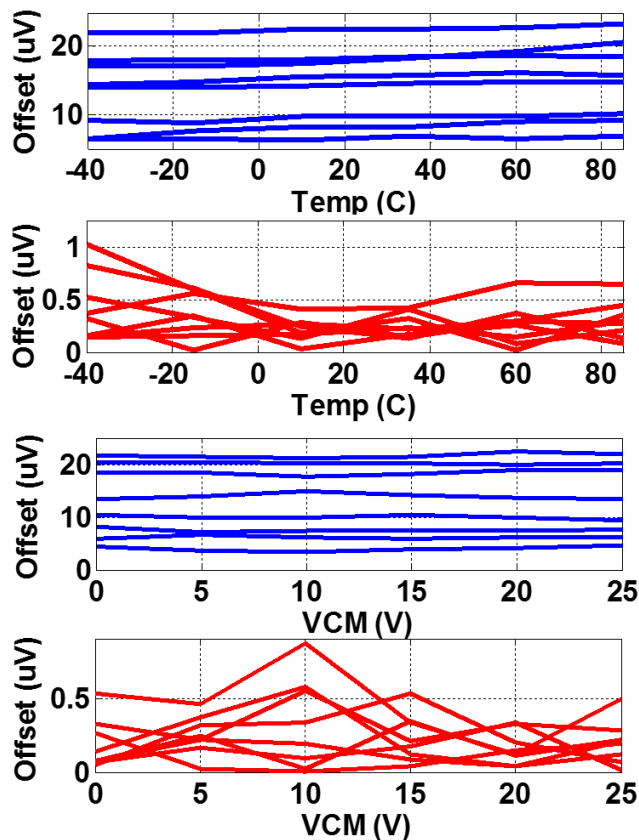


Fig. 12. Offset before CHL (blue) and after CHL (red) over temperature and input CM range.

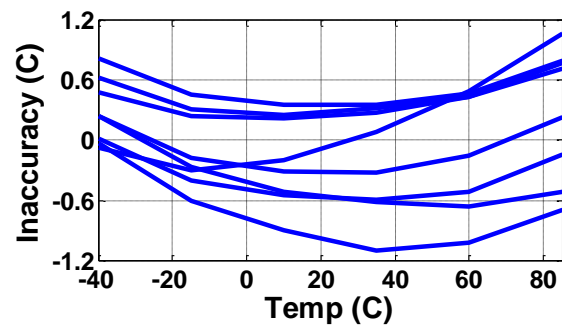


Fig. 13. Temperature sensing error.

TABLE I  
PERFORMANCE SUMMARY AND COMPARISON

	ICMR	I range	$T_{Conv}$ (ms)	SNR (dB)	Gain error (%)	Power	FoM* (dB)
<b>This work</b>	<b>25V</b>	<b>±12A</b>	<b>12.5</b>	<b>72</b>	<b>0.35</b>	<b>25μW</b>	<b>137</b>
[3]	0.75V	±36A	18	67.4	0.3	19.5μW	132
[4]	25V	±4A	2.5	79	0.9	16.4μW	149
[5]	36V	±10A	8.2	69	0.5**	1.5mW	--
[6]	30V	10mA	--	--	0.1***	1mW	--

\* FoM =  $SNR + 10 \log(1/(Power \times 2T_{Conv}))$

\*\* Uses a custom low-TC shunt

\*\*\* One sample is measured only at room temperature

#### IV. CONCLUSION

A shunt-based high-side current sensor has been implemented in a 0.18μm HV BCD process. The beyond-the-rails ADC enables direct digitization of small differential signal in the presence of large CM voltage and hence reduces the power and chip area of HV interface circuits. Thanks to the hybrid TCS, the temperature sensor is greatly simplified due to the relaxed requirement on its accuracy. Based on these two techniques, the sensor achieves the state-of-the-art accuracy with 3x better power efficiency compared to previous work.

#### ACKNOWLEDGMENT

The authors would like to thank Zuyao Chang for his support on chip-on-board bonding.

#### REFERENCES

- [1] Maxim Integrated, MAX44284 Data Sheet. Accessed on March 26, 2018. <<https://datasheets.maximintegrated.com/en/ds/MAX44284.pdf>>
- [2] L. Xu, Burak Gönen, Qinwen Fan, J. H. Huijsing, and K. A. A. Makinwa, "A 110dB SNR ADC with ±30V Input Common-Mode Range and 8μV Offset for Current Sensing Applications," *ISSCC Dig. Tech. Papers*, pp. 374-375, Feb. 2015.
- [3] S. H. Shalmany, Dieter Draxelmayr, and K. A. A. Makinwa, "A ±36A Integrated Current-sensing System with 0.3% Gain Error and 400μA Offset from -55°C to +85°C," *IEEE J. Solid-State Circuits*, vol. 52, no. 4, pp. 1034-1043, Apr. 2017.
- [4] L. Xu, J. H. Huijsing, and K. A. A. Makinwa, "A ±4A high-side current sensor with 25V input CM range and 0.9% gain error from -40°C to 85°C using an analog temperature compensation technique," *ISSCC Dig. Tech. Papers*, pp. 324-325, Feb. 2018.
- [5] Texas Instruments, INA260 Data Sheet. Accessed on March 26, 2018. <<http://www.ti.com/lit/ds/symlink/ina260.pdf>>
- [6] H. Yeom and B. Bakkloglu, "0-30 V Common Mode Range, 120 dB CMRR, and 10 nV/√Hz Noise Floor Current Shunt Monitor IC with an Embedded ΣΔ Modulated Digital Interface," *Analog Integr. Circ. Sig. Process.*, vol. 73, Oct. 2012, pp. 339-351.